JOURNAL OF GEOPHYSICAL RESEARCH, VOL. 103, NO. D13, PAGES 16,703–16,711, JULY 20, 1998

Shipboard measurements of dimethyl sulfide and SO_2 southwest of Tasmania during the First Aerosol Characterization Experiment (ACE 1)

Warren J. De Bruyn,[1] Timothy S. Bates,[2] Jill M. Cainey,[3,4] and Eric S. Saltzman[1]

Abstract. Measurements of seawater dimethylsulfide (DMS), atmospheric dimethylsulfide, and sulfur dioxide (SO_2) were made on board the R/V *Discoverer* in the Southern Ocean, southeast of Australia, as part of the First Aerosol Characterization Experiment (ACE 1). The measurements covered a latitude range of 40°S-55°S during November-December 1995. Seawater DMS concentrations ranged from 0.4 to 6.8 nM, with a mean of 1.7 ± 1.1 nM (1σ). The highest DMS concentrations were found in subtropical convergence zone waters north of 44°S, and the lowest were found in polar waters south of 49°S. In general, seawater DMS concentrations increased during the course of the study, presumably due to the onset of austral spring warming. Atmospheric DMS concentrations ranged from 24 to 350 parts per trillion by volume (pptv), with a mean of 112 ± 61 pptv (1σ). Atmospheric SO_2 was predominantly of marine origin with occasional anthropogenic input, as evidenced by correlation with elevated ^{222}Rn and air mass trajectories. Concentrations ranged from 3 to 1000 pptv with a mean of 48.8 ± 149 pptv (1σ) and a median 15.8 pptv. The mean SO_2 concentration observed in undisturbed marine air was 11.9 ± 7.6 pptv (1σ), and the mean DMS to SO_2 ratio in these conditions was 13 ± 9 (1σ). Diurnal variations in SO_2 were observed, with a daytime maximum and early morning minimum in agreement with model simulations of DMS oxidation in the marine boundary layer. Steady state calculations and photochemical box model simulations suggest that the DMS to SO_2 conversion efficiency in this region is 30-50%. Comparison of these results with results from warmer regions suggests that the DMS to SO_2 conversion efficiency has a positive temperature dependence.

1. Introduction

Sulfur dioxide is the principle precursor for atmospheric sulfate aerosols on a global basis. Sulfur dioxide (SO_2) has both natural and anthropogenic sources, including volcanic emissions, oxidation of biogenic reduced sulfur emissions and combustion of fossil fuels [*Bates et al.*, 1992]. Over the oceans, the major source of sulfur dioxide is believed to be the oxidation of dimethyl sulfide (DMS), which is produced as a result of the metabolic activity of many species of phytoplankton [*Keller et al.*, 1989]. In the atmosphere, SO_2 can form new particles via oxidation to sulfuric acid, followed by homogeneous nucleation with water vapor and possibly other trace substances like ammonia [*Warneck*, 1988]. SO_2 can also contribute to the growth of existing aerosols via heterogeneous oxidation, or by gas-phase oxidation to sulfuric acid, followed by condensation. Sulfate aerosols scatter incoming radiation and alter the albedo of clouds, affecting the radiation balance of the Earth and global climate [*Shaw*, 1983; *Charlson et al.*, 1987].

The gas-phase oxidation of DMS is a complicated process which is still not well understood [*Hynes et al.*, 1986; *Barone et al.*, 1996; *Yin et al.*, 1990a, b; *Turnipseed and Ravishankara*, 1993]. Because of this complexity, it is important to compare models derived from laboratory data with observed distributions of DMS and its oxidation products in the atmosphere. The current database for atmospheric sulfur compounds in marine air consists primarily of measurements of DMS and its aerosol products, sulfate and methanesulfonate. In recent years, improved analytical instruments have made it possible to begin to study various intermediates, including SO_2, dimethyl sulfoxide (DMSO), and dimethyl sulfone ($DMSO_2$) at remote sites [*Bandy et al.*, 1992; *Putaud et al.*, 1992; *Berresheim et al.*, 1993; *Bandy et al.*, 1996; *Yvon and Saltzman*, 1996; *Ayers et al.*, 1996]. An expanded database for these species is needed to test current models of DMS oxidation and to fully understand the mechanisms by which the DMS oxidation process impacts marine aerosol production and growth.

Here we report high time resolution SO_2 and DMS measurements made on board the R/V *Discoverer* in the Southern Ocean south of Tasmania. These measurements were carried out from November 15, 1995, to December 13, 1995 as part of the International Global Atmospheric Chemistry (IGAC) program's First Aerosol Characterization Experiment (ACE 1). The data are examined using simple steady state and time-dependent gas-phase photochemical box models, and the implications for the DMS oxidation mechanism are discussed.

[1]Rosenstiel School of Marine and Atmospheric Science, University of Miami, Miami, Florida.

[2]Pacific Marine Laboratory, NOAA, Seattle, Washington.

[3]CSIRO Atmospheric Research, Aspendale, Australia.

[4]New Zealand Institute for Water and Atmospheric Research Ltd., Kilbirnie, Wellington, New Zealand.

Paper number 98JD00971.
0148-0227/98/98JD-00971$09.00

2. Experiment

2.1. Dimethylsulfide

DMS air samples were collected through a Teflon line which ran approximately 60 m from the top of the aerosol sampling mast (17 m above sea level, forward of the ship's bridge) to the analytical system. One hundred mL min^{-1} of the 4 L min^{-1} flow were pulled through an aqueous KI solution at the analytical system to eliminate oxidant interferences [*Saltzman and Cooper*, 1988]. The air sample volume ranged from 0.5 to 1.5 L depending on the DMS concentration. Seawater samples were collected from the ship's seawater pumping system at a depth of 5 m. The seawater line ran to the analytical system where 5.1 mL of sample were valved into a teflon gas stripper. The samples were purged with hydrogen at 80 mL min^{-1} for 5 min. Water vapor in both the air and water samples was removed by passing the flow through a -25°C Teflon tube filled with silanized glass wool. DMS was then trapped in a -25°C Teflon tube filled with Tenax. During the sample trapping period, 6.2 pmol of methylethyl sulfide were valved into the hydrogen stream as an internal standard. At the end of the sampling/purge period, the coolant was pushed away from the trap, and the trap was electrically heated. DMS was desorbed onto a DB-1 mega-bore fused silica column where the sulfur compounds were separated isothermally at 50°C and quantified with a sulfur chemiluminesence detector. The detection limit during ACE 1 was approximately 0.8 pmol. The system was calibrated using gravimetrically calibrated permeation tubes. The precision of the analysis, based on both replicate analyses of a single water sample and replicate analyses of a standard introduced at the inlet of the air sample line, was typically ±8%. The performance of the system was monitored regularly by running blanks and standards through the entire system. Values reported here have been corrected for recovery losses. System blanks were below the detection limit. One atmospheric DMS measurement was made every 30 min.

2.2. Sulfur Dioxide

Sulfur dioxide was measured using an HPLC/fluorescence technique with pre-column derivatization. Details of the instrument design and performance are discussed by *Saltzman et al.* [1993] and *Gallagher et al.* [1997]. Here we briefly describe the principles of operation of the instrument and its performance during this experiment.

Ambient air was drawn into the instrument through a coarse Teflon filter to remove particulates, a nafion membrane dryer to remove water vapor and a gas-liquid exchange coil. All gas lines up to and including the entrance to the nafion dryer were heated to 50°C to prevent the condensation of water vapor and resultant loss of SO_2. In the gas-liquid exchange coil, SO_2 was absorbed from the ambient air stream into an aqueous formaldehyde scrubbing solution (10μM, pH=4.6). The scrubbing solution was mixed serially with 1mM ethanolamine in a pH 9 borate buffer, 1.1 mM orthopthalaldehyde (OPA), and a sodium acetate solution (2.5 M) buffered at pH 5.7. The pH 9 buffer converts the liquid-phase SO_2 to sulfite, which reacts with the ethanolamine and OPA to form a stable, highly fluorescent iso-indole derivative. The resultant mixture flows through a delay coil (2 min) to optimize the derivative yield. The sodium acetate solution is added to lower the pH of the sample, slowing further reaction of the derivative with OPA and reducing degradation of the HPLC column material. The reaction stream flows through a 600 µL injection loop, which was periodically injected into an isocratic reverse-phase (Spherisorb C-18) column. The isoindole derivative was detected by fluorescence at 380 nm (λ_{ex} = 330nm; Hitachi F1000 or Hitachi L7480).

The instrument used a calibration system based on the double dilution of an SO_2 permeation device, in which the analyte never passes through a mass flow controller. Using a 12 ng min^{-1} device, the calibration system can generate gas-phase standards ranging from 3 to 600 pptv. During the cruise, ambient air was analyzed continuously, except during calibration periods and periods of instrument maintenance and obvious adverse wind direction. Calibrations were run daily, and SO_2 loss in the inlet was monitored by adding standards to the inlet before the particle filter. The inlet was cleaned, and the particle filter was changed whenever SO_2 loss became significant (>15%). Blanks were generated by scrubbing ambient air with carbonate filters and were run 4-5 times a day.

The system is fully automated, has a linear response over the normal range of atmospheric concentrations, a 4 min sample integration time, and a 7 min measurement period. The instrument has a 3-5 pptv detection limit (3σ of the daily mean blank), and the precision is estimated to be less than 10% at 20 pptv. The detection limit achieved during this project represents an improvement over that recently reported by *Gallagher et al.* [1997]. This improvement was achieved by using lower reagent concentrations, which resulted in a lower system blank. In Figure 1, we show chromatograms for a blank, a 5 pptv, a 17 pptv, and a 30 pptv air sample.

During this project, the instrument was positioned in an air-conditioned van on the starboard side of the flying bridge well forward of the stack, and ambient air was sampled directly through a removable port on the forward wall of the van. The van was approximately 17 m above sea level. Elevated SO_2 levels associated with stack gases were observed during episodes of low or highly variable wind speed and direction, relative to the motion of the ship. Contaminated samples have been filtered from the data set using shipboard wind speed and direction. Stack gas

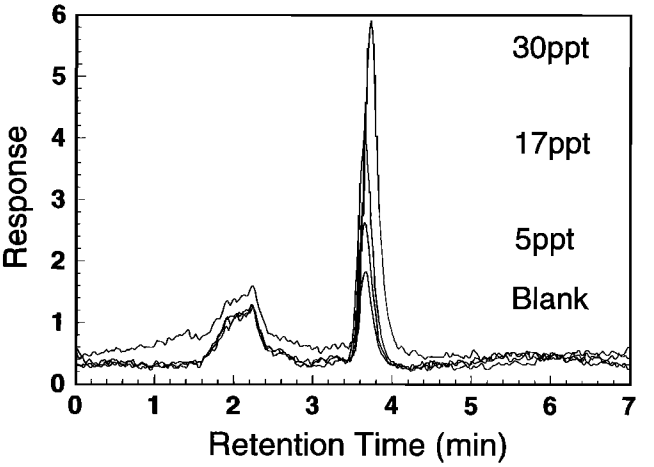

Figure 1. Typical SO_2 chromatograms for ambient air containing 5, 17 and 30 pptv SO_2. The blank is ambient air passed through a carbonate filter.

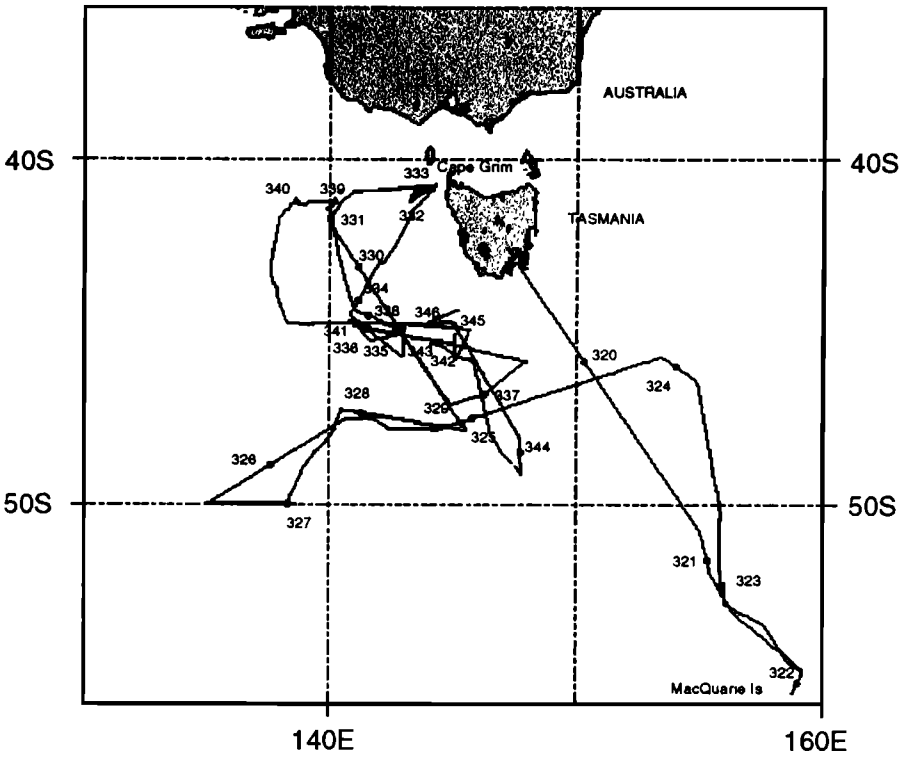

Figure 2. The R/V *Discoverer* cruise track during ACE 1. The numbers represent the ship position at the beginning of each day, where the number is the day of year in 1995.

contamination was particularly severe when the ship steamed downwind in order to conduct balloon releases and tracking exercises associated with the ACE 1 Legrangian experiment [*Bates et al.*, this issue (b)]. The SO_2 data are 30 min averages around each DMS measurement. Each SO_2 point is therefore an average of approximately three measurements.

3. Results

The ACE 1 *Discoverer* cruise was carried out southeast of Australia in the region bounded by 40°-55°S and 135°-160°E (Figure 2). For most of the study period, the *Discoverer* occupied a region southwest of Tasmania. The cruise track was dictated by several objectives in addition to the study of gas-phase sulfur chemistry, including carrying out an oceanographic survey of the region, providing logistical support of the MacQuarie Island field site, and releasing balloons for airborne chemistry studies. Consequently, the ship often experienced following winds, which are unsuitable for SO_2 measurement due to the potential for stack gas contamination. As a result, SO_2 data are sparse during portions of the field study. Measurements of seawater DMS, atmospheric DMS and SO_2, and several additional environmental parameters are shown as a function of time during the cruise in Figure 3.

The study region was comprised of three distinct water mass types identified on the basis of shipboard salinity and temperature measurements [*Bates et al.*, this issue (a); F. B. Griffiths et al., unpublished manuscript, 1998]. The northernmost end of the cruise track (40°-43°S) was located in the subtropical convergence zone (salinity >34.8). The southernmost end of the cruise track (49°-55°S) was in colder, fresher polar waters (salinity <34.2). Most of the cruise was carried out in Subantarctic waters (43°-49°S). This region was intermediate between the subtropical convergence zone and polar waters in terms of temperature and salinity. The Subantarctic waters were apparently heterogeneous, as evidenced by variability in salinity.

The study region is located in the westerlies, and meteorological conditions during this study were affected by numerous low-pressure systems and cold fronts. According to *Hainsworth et al.* [this issue], frontal activity was somewhat more active than normal during the period of the ACE 1 study, due to the presence of a long wave trough west of the study area. This trough moved to the east through the region during the course of this cruise. Frontal systems typically passed through the region every few days, as shown in the time series of atmospheric surface pressure shown in Figure 3. Of particular note is the passage of a cold front during day 337, which was followed by several days of clear, high-pressure conditions.

The oceanographic setting is clearly reflected in the seawater DMS concentrations, shown in Figure 3. The seawater DMS concentrations were generally lowest in the polar waters (<1 n*M*) and highest in the subtropical convergence zone (2-7 n*M*). The DMS concentrations in Subantarctic waters ranged from 1-5 n*M*, with the lowest concentrations occurring early in the cruise, and the highest concentrations occurring late in the study. This increase may reflect the onset of the seasonal increase in biological productivity during austral spring.

Atmospheric DMS concentrations ranged from 24 to 350 pptv, with a mean of 112 ± 61 pptv (1σ, n = 542). As with seawater DMS, the lowest atmospheric concentrations were observed near the beginning of the cruise, in polar waters, and the highest were observed in the subtropical convergence zone

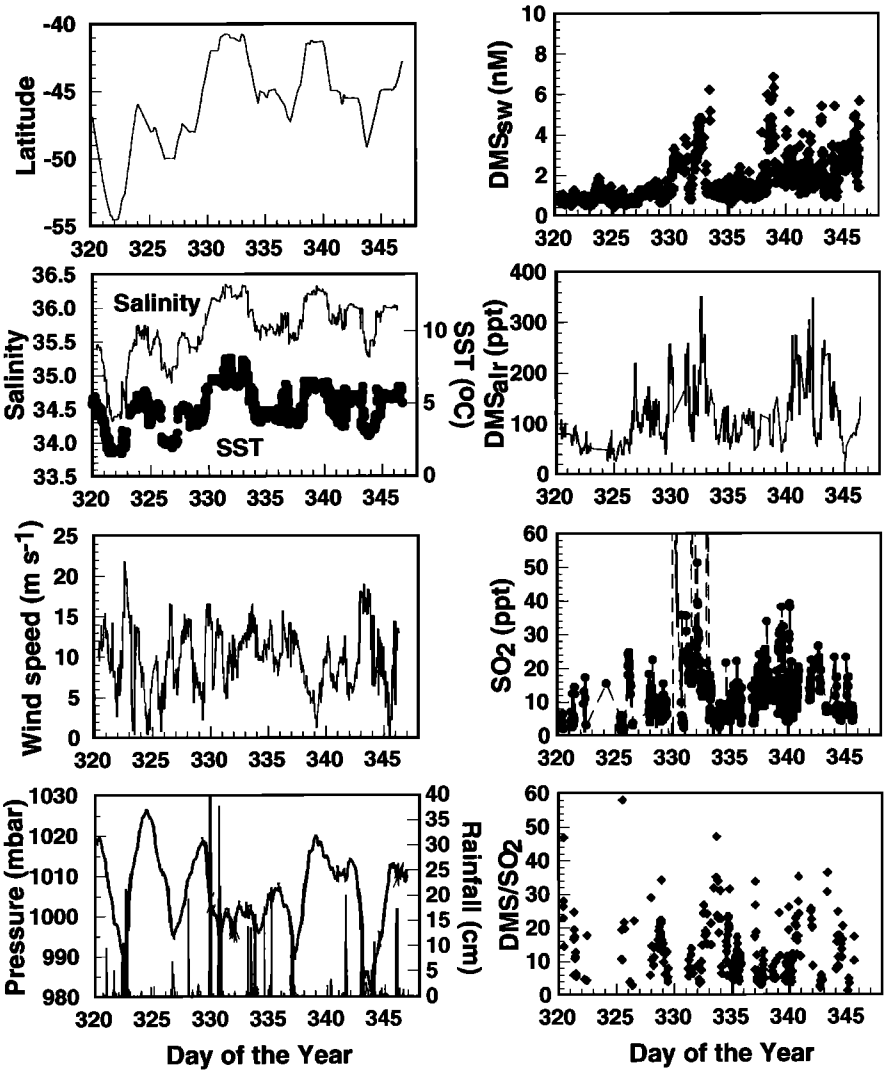

Figure 3. Time series of various parameters measured during the ACE 1 cruise in the Southern Ocean aboard the R/V *Discoverer*. (left from top) Latitude, salinity and sea surface temperature, wind speed, atmospheric pressure, and rainfall. (right from top) Seawater DMS, atmospheric DMS, atmospheric SO_2, and atmospheric DMS/SO_2 ratios.

and in the Subantarctic water late in the cruise. Atmospheric DMS levels should be a function of several parameters in addition to seawater DMS concentrations, including OH concentrations; temperature (insofar as it affects reaction rates); boundary layer height; vertical exchange between the boundary layer and free troposphere; and wind-driven turbulence as it affects air/sea exchange. *Bates et al.* [this issue (a)] estimated the DMS fluxes from this data based on the shipboard measurements of wind speed and water temperature. One possible notable example of the strong influence of wind speed on gas emissions is on days 338-339, when seawater DMS concentrations reached a maximum for the entire cruise of 7 n*M*, an increase of a factor of 5 over previous concentrations. This increase was barely detectable in atmospheric DMS levels, possibly because it coincided with the onset of a high-pressure system associated with very low wind speeds. The low atmospheric DMS levels could also be a result of possible dilution of boundary layer air by subsiding DMS free air.

Atmospheric SO_2 concentrations ranged from 1 pptv to more than 1000 with a mean of 48.8 ± 149 pptv (1σ). There were four episodes during which continentally influenced air masses reached the ship [*Bates et al.*, this issue (a)]. These were days 330, 332, 333, and 343. During these episodes, ^{222}Rn levels reached over 100 mBq/m^3, and SO_2 concentrations were elevated over background conditions, ranging up to 1000 pptv. There were also several episodes where the ship encountered rain and SO_2 levels were suppressed. In general, the highest levels of SO_2 were observed while the ship was either in the subtropical convergence zone or in the Subantarctic waters during periods of high seawater DMS concentrations. Eliminating the data with elevated ^{222}Rn levels yields a mean SO_2 concentration of 11.9 ± 7.6 pptv for undisturbed marine air.

Overall, the atmospheric DMS and SO_2 measurements reported here are consistent with the average weekly SO_2 and DMS measurements made by *Ayers et al.* [1996] between 1990 and 1993 at Cape Grim. For the months of November and December, respectively, *Ayers et al.* [1996] report mean DMS concentrations of 111 and 160 pptvv, and mean SO_2 concentrations of 8 and 12 pptv.

In order to examine the relationship between DMS and SO_2 we have calculated the DMS/SO_2 ratio for each 30 min sample. Ratios were not calculated for samples associated

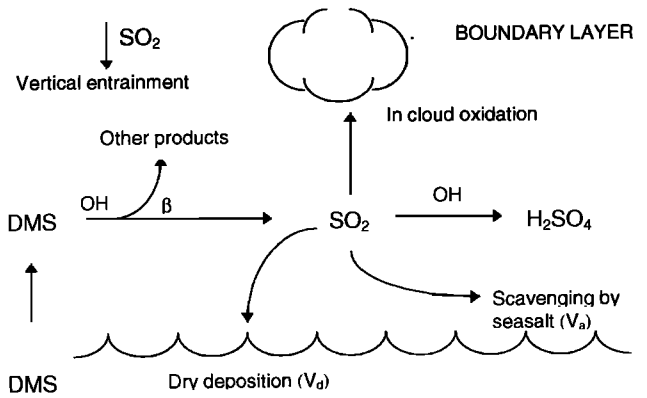

Figure 4. Sulfur dioxide budget in the remote marine boundary layer.

with high ^{222}Rn levels or rainfall. The resulting DMS/SO_2 ratios range from 0 to 60, with a median of 11 and a mean of 13 ± 9 (1σ, n = 244).

4. Discussion

4.1. DMS/SO_2 Ratios

Figure 4 illustrates the processes involved in the cycling of DMS and SO_2 in the marine boundary layer. DMS enters the boundary layer via gas exchange across the sea surface and is lost primarily by gas-phase reaction with OH. Some DMS is also lost from the boundary layer by detrainment to the free troposphere. Sulfur dioxide enters the remote boundary layer from the oxidation of DMS and via vertical entrainment from the free troposphere. The main removal processes for SO_2 are homogeneous OH oxidation to produce H_2SO_4, heterogeneous loss to in-cloud oxidation, heterogeneous scavenging by sea-salt aerosols, and dry deposition to the sea surface. Episodically, uptake by rain droplets also removes SO_2 from the atmosphere. A steady state expression for the relationship between atmospheric DMS and SO_2 can be written as follows, assuming that vertical entrainment of SO_2 is small relative to SO_2 produced by DMS oxidation:

$$\frac{[DMS]}{[SO_2]} = \frac{(f_a + f_c + v_d/H + k_{SO_2}[OH])}{\beta k_{DMS}[OH]} \quad (1)$$

where f_a is the first-order loss of SO_2 to sea-salt aerosols, f_c is the first-order loss of SO_2 to in-cloud oxidation, V_d is the dry deposition velocity for SO_2 to the sea surface, H is the boundary layer height, β is the efficiency of SO_2 production, k_{DMS} is the DMS+OH bimolecular rate constant, and k_{SO2} is the SO_2+OH bimolecular rate constant. Equation (1) is valid as long as the average SO_2 level is close to the average steady state SO_2 concentration, which is true as long as the time required to reach steady state is short relative to the timescale of the experiment and perturbations to the system. The relatively long periods of time in which the SO_2 levels did not change significantly suggest that this is the case.

DMS/SO_2 ratios measured in this study are higher than those observed in recent studies in the tropics and subtropics [*Bandy et al.*, 1996; W.J. De Bruyn et al., manuscript in preparation, 1997]. As can be seen in equation (1), higher DMS/SO_2 ratios should be associated with greater SO_2 production rates and/or larger SO_2 sinks. The SO_2 production rate is a function of the SO_2 production efficiency which is currently unknown. Estimates for β vary widely depending on assumptions about the details of the DMS oxidation mechanism [*Bandy et al.*, 1992; *Barone et al.*, 1995; *Ayers et al.*, 1997]. By estimating the values of various parameters in this steady state expression, we can use the measured DMS/SO_2 ratios to estimate β.

Values for the parameters in equation (1), calculated from regional averages of measurements or obtained from the literature, are given in Table 1. Dry deposition velocities for SO_2 to the sea surface were calculated using the relationship $V_d = 1.22 \times 10^{-3} U$ [*Yvon et al.*, 1996] where U is the wind speed in m s^{-1}. The bimolecular rate constant k_{DMS} was taken from *Hynes et al.* [1986], and the hydroxyl radical concentration is the regional average recommended by *Spivakowsky et al.* [1990]. The in-cloud oxidation rate was estimated from the work of *Hegg* [1995], and the bimolecular rate constant k_{SO2} was taken from *DeMore et al.* [1992]. The scavenging of SO_2 by sea-salt aerosols was estimated from the non-sea-salt sulfate concentrations in coarse mode aerosols measured on the R/V *Discoverer* [*Bates et al.*, this issue (a)] assuming a 1-2 day lifetime for these aerosols. Using the values in Table 1, we estimate that it would require an SO_2 production efficiency of 33-42% to support the observed average DMS/SO_2 ratio. This is lower than production efficiencies observed in the tropics and subtropics [*Bandy et al.*, 1996; W.J. De Bruyn et al., manuscript in preparation, 1997].

Table 1. Regional Average or Calculated Values of Parameters Controlling Steady state DMS/SO_2 Ratios and the Resultant Yield of SO_2 Required to Support Observed Ratios

Parameters	Value	Source
Temperature	9.2 °C	R/V Discoverer
Wind	9.73 m s^{-1}	R/V Discoverer
OH	550,000 mol cm^{-3}	Spivakowsky et al. [1990]
H	100,000 cm	
V_d	1.19 cm s^{-1}	$V_d = 1.25 \times 10^{-3} U$ [Liss, 1983; Hicks and Liss, 1976]
V_d/H	1.19×10^{-5} s^{-1}	
f_c	1.2×10^{-6} s^{-1}	Hegg [1985]
$k_{SO2}[OH]$	3.83×10^{-7} s^{-1}	DeMore et al. [1992]
$k_{DMS}[OH]$	4.28×10^{-6} s^{-1}	Hynes et al. [1986]
f_a	$1.6\text{-}3.2 \times 10^{-3}$ mol cm^{-3} s^{-1} ($4.96\text{-}9.92 \times 10^{-6}$ s^{-1})	
β	0.33-0.42	

The uncertainty in this estimation of β is dominated by the uncertainty in the calculation of the SO_2 sea-salt scavenging rate. As mentioned above, the estimation given in Table 1 is based on non-sea-salt concentrations measured in coarse aerosols on board the R/V *Discoverer*. On the basis of the concentration of non-sea-salt sulfate measured in large aerosols at Cape Grim during ACE 1, H. Sievering et al. (personal communication, 1997) calculate a non-sea-salt sulfate flux to the ocean of 1 umol $m^{-2} d^{-1}$ which is equivalent to an SO_2 sink of 7.0 x 10^{-3} mol cm^{-3} s^{-1}. This is more than a factor of 2 greater than the scavenging rate estimated from the aerosol measurements made on the R/V *Discoverer* and would require an SO_2 production efficiency of 60% to support the observed DMS/SO_2 ratios. An additional source of uncertainty is the assumption that the vertical entrainment of SO_2 is negligible. Aircraft measurements (A. R. Bandy et al., unpublished manuscript, 1998) during ACE 1 show that, on average, the concentration of SO_2 in the free troposphere was not significantly higher than the concentration in the boundary layer, suggesting that this assumption is reasonable. However, there were clearly days when concentrations could have been as much as a factor of 2 higher in the free troposphere. If free tropospheric concentrations were always a factor of 2 higher than boundary layer levels and the SO_2 exchange velocity was 0.5 cm s^{-1}, including the resultant entrainment flux in the above calculation would lower the conversion efficiencies in Table 1 to 24-33%. An alternative approach to assessing the SO_2 production efficiency and total SO_2 sink is to look at time-dependent variations in the data. This approach allows for an independent assessment of the total SO_2 sink from the data.

4.2. Diurnal Variations in SO_2

In general, SO_2 should exhibit a consistent diurnal variation in the marine boundary layer, with a maximum in the late afternoon reflecting the photochemical oxidation of DMS, and a minimum at dawn resulting from nighttime losses due to heterogeneous processes. Assuming that vertical entrainment is negligible, the nighttime loss is a direct measure of the total SO_2 sink. This diurnal variability in SO_2 was recently observed at a tropical site on Christmas Island [*Bandy et al.*, 1996] and during a transect prior to the ACE-1 intensive (W.J. De Bruyn et al., manuscript in preparation, 1997). Analysis of that data suggested SO_2 production efficiencies of 60-80% and total deposition velocities for SO_2 of 0.7-1 cm s^{-1}.

The Southern Ocean is an environment in which one might not expect to find highly reproducible diurnal cycles because of the rapidly changing meteorological conditions, and the high degree of spatial variability in the sea surface DMS source. In addition, the cruise track required for nonphotochemical ACE 1 goals precluded long sampling periods in steady conditions. However, in spite of these factors the expected diurnal variation in the SO_2 data was often observed during this study. In Figure 5a, we show SO_2 data with a clear afternoon maximum and early morning minimum for a 3.5 day period (days 337.5-341) during the experiment. The solid lines in the figure are a plot of solar irradiance. The difference in absolute SO_2 levels and amplitude of the diurnal cycle between days 338 and days 339-340 is due to varying oceanographic and meteorological conditions. On day 338, the *Discoverer* steamed northeast through Subantarctic waters under cloudy skies, while for most of days 339 and 340 the *Discoverer* was stationed southwest of Cape Grim in the subtropical convergence zone in a well defined cloud-free high-pressure system (Figures 1 and 2). Day 338 is more representative of average conditions encountered for the ACE 1 intensive. Interestingly, atmospheric DMS did not exhibit consistent diurnal cycles during this period. This may reflect the heterogeneity of nearby sources and/or the longer lifetime of DMS.

In Figures 5b and 5c, the SO_2 data for days 338 and 339-340 have been averaged into 2 hour bins over a 24 hour period and compared to the output from a time-dependent photochemical box model. Error bars are standard errors of the mean. The photochemical box model simulates the photochemistry of the marine boundary layer using a multistream radiation code, 11 photolysis reactions, and 140 thermal reactions. The model includes detailed OH chemistry and has previously been described in detail by *Yvon and Saltzman* [1993] and *Yvon et al.* [1996]. The values of various input parameters and their sources are given in Table 2. Wind speeds, temperature, relative humidity, ozone, and carbon monoxide were measured aboard the R/V *Discoverer* (J. Johnson et al., personal communication, 1997). Methane levels were regional averages obtained from *Koga and Tanaka* [1993] and *Spivakovsky et al.* [1990] and total column ozone levels were obtained from *Spivakowsky et al.* [1990]. Total NO_x levels were assumed to be 20 pptv. Radiosondes released approximately every 3 hours suggest an average boundary layer height of 1 km ($1\sigma/n^{1/2}$~0.08 km). Dry deposition velocities for SO_2 to the sea surface were once again calculated from the relationship V_d=1.22 x10^{-3}U [*Yvon et al.*, 1996] were U is the wind speed in m s^{-1}. Using these conditions, the model generated midday maximum OH concentrations of 2.8 x 10^{-6} molecules cm^{-3}, which were in reasonable agreement with airborne measurements of OH made in this region by F. Eisele et al. (personal communication, 1997).

For these simulations, the DMS flux into the boundary layer was adjusted until the model produced results which agreed with the observed average DMS levels. Fluxes of 3.2 and 5.4 umol $m^{-3}d^{-1}$ were required to support the observed atmospheric DMS levels on days 338 and 339-340 respectively. These fluxes are consistent with fluxes calculated from measured seawater DMS levels [*Bates et al.*, this issue (a)]. Based on aircraft measurements of SO_2 and DMS (A. R. Bandy et al., unpublished manuscript, 1998) above the boundary layer, vertical exchange in the model has once again been assumed to be negligible. The production efficiency for SO_2 and the loss of SO_2 to sea-salt aerosols were then adjusted to obtain the best agreement between the model simulations and the observed diurnal variations in SO_2. These two parameters exert opposite effects on the simulated SO_2 diurnal profile, but they do so in slightly different ways. Varying the production efficiency alters the daytime-only production of SO_2. The aerosol sink is assumed to be non-photochemical and constant throughout the day and night. Furthermore, the aerosol sink is assumed to be limited by the alkalinity of sea-salt aerosols [*Chameides and Stelson*, 1992], and therefore zero-order in SO_2.

For day 338, reasonable agreement is obtained with SO_2 production efficiencies of 30-40% and an aerosol sink of 3.7-5.6 x 10^3 molecules cm^{-3} s^{-1}. Reasonable agreement is obtained for days 339-340 with production efficiencies of 40-50% and an aerosol sink of 1-1.3x10^4 mol cm^{-3} s^{-1}. Once again these production efficiencies are less than observed in

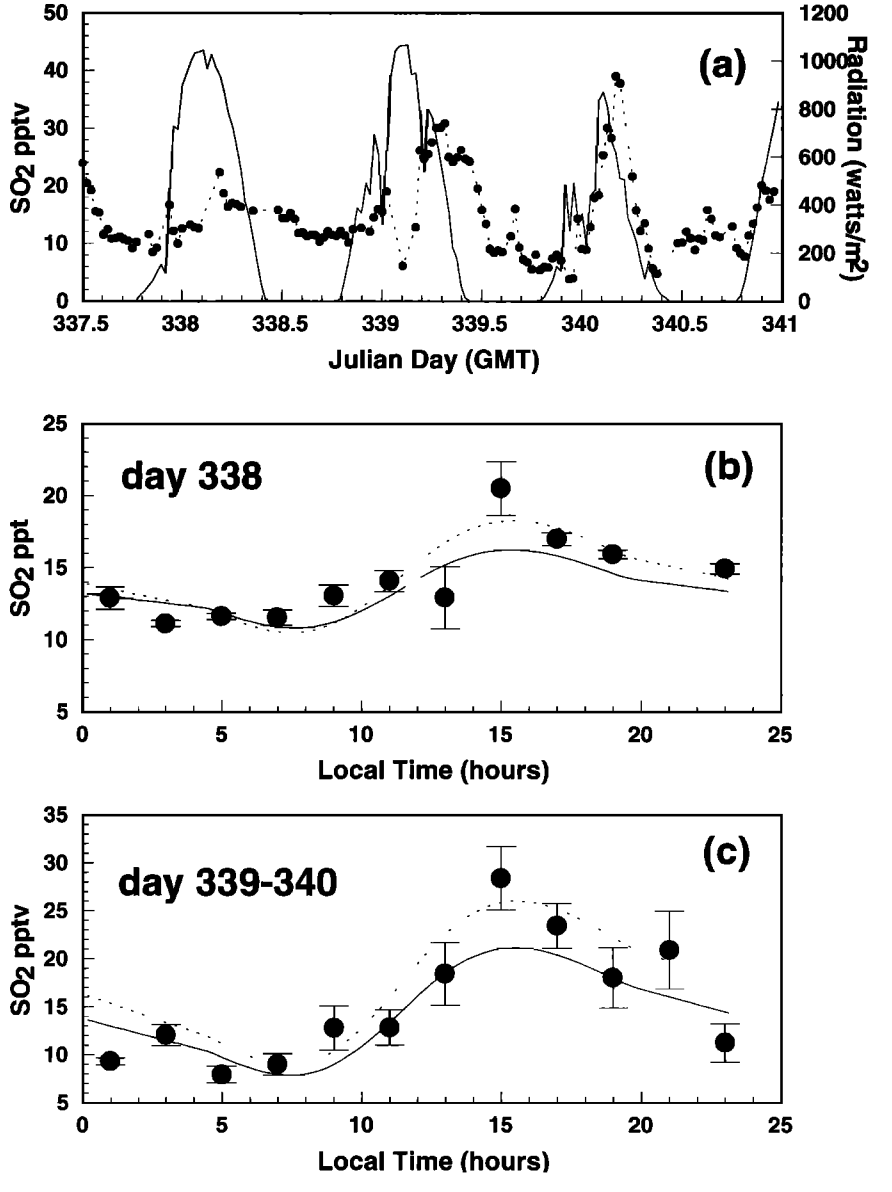

Figure 5. (a) Measured sulfur dioxide levels for Julian days 337.5 to 341. The solid lines are solar radiation. (b) SO_2 data for Julian day 338 averaged into 2 hour bins. The curves are photochemical box model output. The dashed curve was obtained with an SO_2 production efficiency of 40% and an aerosol sink of 5.6 x 10^3 molecules cm^{-3} s^{-1}, and the solid curve was obtained with a production efficiency of 30% and an aerosol sink of 3.7 x 10^3 molecules cm^{-3} s^{-1}. (c) SO_2 data for Julian days 339 and 340 averaged into 2 hour bins over a single 24 hour period. The curves are photochemical box model output. The dashed curve was obtained with a production efficiency of 50% and an aerosol sink of 1.3 x 10^4 molecules cm^{-3} s^{-1}, and the solid curve was obtained with a production efficiency of 40% and an aerosol sink of 1 x 10^4 molecules cm^{-3} s^{-1}.

Table 2. Input Parameters for Photochemical Model Calculations.

Parameter			Source
Julian day	338	339-340	R/V *Discoverer*
Latitude	42.6°S	42.5°S	R/V *Discoverer*
Wind speed, m s^{-1}	5.87	6.90	R/V *Discoverer*
Vd, cm s^{-1}	0.71	0.84	
Temperature, °C	10.2	11.3	R/V *Discoverer*
Relative Humidity, %	66	74	R/V *Discoverer*
O_3, ppb	20	20	J. Johnson et al. (personal communication, 1998)
CO, ppb	60	60	Koga and Tanaka [1993]; Kok et al., [this issue]
CH_4, ppm	1.63	1.63	Koga and Tanaka [1993]; Spivakowsky et al.[1990]
Total O_3, mmol m^{-2}	320	320	Spivakowsky et al.[1990]
NO_x, pptv	20	20	estimated
Boundary height, km	1	1	

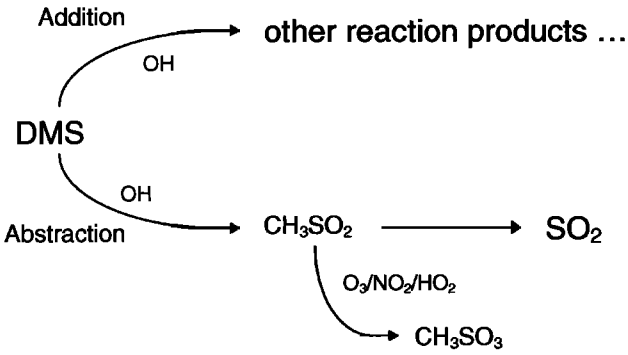

Figure 6. A simplified DMS oxidation scheme.

the tropics [*Bandy et al.*, 1996; W.J. De Bruyn et al., manuscript in preparation, 1997). The aerosol sink on day 338 agrees well with the aerosol sinks calculated from the average measured non-sea-salt sulfate concentrations in coarse mode aerosols on the R/V *Discoverer* and at Cape Grim. The loss rate of SO_2 to sea-salt aerosols can be converted into a deposition velocity using the boundary layer height and mean SO_2 concentration. The sinks obtained from the model simulations are equivalent to deposition velocities of 0.97-1.5 cm s^{-1} and 2.0-2.6 cm s^{-1} for days 338 and 339-340, respectively. This is significantly larger than the estimated loss to the sea surface of 0.71 and 0.84 cm s^{-1} for days 338 and 339-340, respectively. Combining both sinks yields a total sink that is significantly larger than estimated sinks for tropical and subtropical studies and an overall SO_2 lifetime of 12.5-16.5 hours on day 338 and 8-10 hours on days 339-340.

4.3. Implications for the Mechanism of DMS Oxidation

In Figure 6, we show a simplified DMS oxidation mechanism highlighting some key features. Laboratory kinetic studies have shown that the initial step in the mechanism proceeds via hydrogen abstraction and OH addition [*Hynes et al.*, 1986; *Barone et al.*, 1996]. It is generally assumed that SO_2 is produced only through the abstraction channel and via the thermal decomposition of the intermediate CH_3SO_2. However, reaction rates of the intermediate CH_3SO_2 and final product yields are poorly known [*Yin et al.*, 1990a]. In this simplified mechanism, the efficiency of SO_2 production is the product of the branching ratio for hydrogen atom abstraction and CH_3SO_2 thermal decomposition.

The SO_2 production efficiencies estimated from this study (30-50%) agree reasonably well with the branching ratio for hydrogen atom abstraction (40%) at the temperatures encountered during this study. Assuming that no SO_2 is produced through the addition channel, a production efficiency of 30% requires that 75% of the abstraction channel produces SO_2. This is consistent with estimates for the branching ratio for the thermal decomposition of CH_3SO_2 [*Barone et al.*, 1995; *Ayers et al.*, 1997]. A production efficiency of 50% would imply that >10% SO_2 is produced through the addition channel.

Field studies in the tropics suggest SO_2 yields of 60-80% at 25°-30°C [*Bandy et al.*, 1996; W. J. De Bruyn et al., manuscript in preparation, 1997]. Yields estimated here of 50% or less at approximately 10°C suggests that the SO_2 production efficiency has a positive temperature dependence. This is consistent with the simplified mechanism given in Figure 6 and current understanding of the DMS oxidation process. Both the addition channel and the CH_3SO_2 thermal decomposition channel should become less important at colder temperatures [*Hynes et al.*, 1986; *Ayers et al.*, 1997; *Barone et al.*, 1995].

5. Summary

Measurements of seawater dimethylsulfide (DMS), atmospheric dimethylsulfide and sulfur dioxide (SO_2) were made on board the R/V *Discoverer* in the Southern Ocean, southeast of Australia as part of the First Aerosol Characterization Experiment (ACE 1). Seawater DMS concentrations ranged from 0.4 to 6.8 nM and increased during the course of the study, presumably due to the onset of austral spring warming. Atmospheric DMS concentrations ranged from 24 to 350 pptv, with a mean of 112 ± 61 pptv (1σ). Atmospheric SO_2 concentrations ranged from 3 to 1000 pptv. The mean "background" SO_2 concentration observed was 11.9 ± 7.6 pptv (1σ), and the mean DMS/SO_2 ratio was 13.2 ± 9.0 (1σ). Diurnal variations in SO_2 were observed, with a daytime maximum and early morning minimum, in good agreement with model simulations of DMS oxidation in the marine boundary layer. Steady state calculations and photochemical box model simulations suggest that the DMS to SO_2 conversion efficiency in this region is 30-50%, which is lower than that estimated for field studies in tropical regions [*Bandy et al.*, 1996; W. J. De Bruyn et al., manuscript in preparation, 1997].

Acknowledgments. This research is a contribution to the International Global Atmospheric Chemistry (IGAC) Core project of the International Geosphere-Biosphere Program (IGBP) and is part of the IGAC Aerosol Characterization Experiments (ACE).

References

Ayers, G.P., J.M. Cainey, H. Graneck and C. Leck, Dimethyl sulfide oxidation and the ratio of methanesulfonate to non sea-salt sulfate in the marine aerosol, *J. Atmos. Chem.*, *25*, 307-325, 1996.

Ayers, G.P., J.M. Cainey, R.W. Gillet, E.S. Saltzman, and M. Hooper, Sulfur dioxide and dimethyl sulfide in the marine air at Cape Grim, 41°S, *Tellus, Ser. B*, *49*, 292-299, 1997.

Bandy, A.R., D.L. Scott, B.W. Blomquist, S.M. Chen, and D.C. Thornton, Low yields of SO_2 from dimethyl sulfide in the marine boundary layer, *Geophys. Res. Lett.*, *19*, 1125-1127, 1992.

Bandy, A.R., D.C. Thornton, B.W. Blomquist, S. Chen, T.P. Wade, J.C. Ianni, G.M. Mitchell, and W. Nadler, Chemistry of dimethyl sulfide in the equatorial Pacific atmosphere, *Geophys. Res. Lett.*, *23*, 741-744, 1996.

Barone, S.B., A. Turnipseed, and A.A. Ravishankara, Role of adducts in atmospheric oxidation of dimethyl sulfide (DMS), *Faraday Discuss.*, *100*, 39-54, 1995.

Barone, S.B., A. Turnipseed, and A.A. Ravishankara, Reactions of OH with dimethyl sulfide (DMS), 1, Equilibruim constant for OH+DMS reaction and the kinetics of OH.DMS +O_2 reaction, *J. Phys. Chem.*, *100*, 14694-14702, 1996.

Bates, T.S., B.K. Lamb, A. Guenther, J. Dignon, and R. E. Stoiber, Sulfur emissions to the atmosphere from natural sources, *J. Atmos. Chem.*, *14*, 315-337, 1992.

Bates, T.S., V.N. Kapustin, P. K. Quinn, D. S. Covert, D. Coffman, C. Mari, P.A. Durkee, W. J. De Bruyn, and E.S. Saltzman, Processes controlling the distribution of aerosol particles in the marine boundary layer during ACE 1, *J. Geophys. Res.*, this issue (a).

Bates, T.S., B.J. Huebert, J.L. Gras, B. Griffiths, and P.A. Durkee, The International Global Atmospheric Chemistry (IGAC) Project's First Aerosol Characterization Experiment (ACE 1): Overview, *J. Geophys. Res.*, this issue (b).

Berresheim, H., Biogenic sulfur emissions from the Subantarctic and Antarctic oceans, *J. Geophys. Res.*, *92*, 13245-13262, 1987.

Berresheim, H., F.L. Eisele, D.J.Tanner, L.M. Mcinnes, D.C. Ramsey-Bell, and D.S. Covert, Atmospheric sulfur chemistry and CCN concentrations over the northeastern Pacific Coast, *J. Geophys. Res.*, *98*, 12701-12711, 1993.

Chameides, W.L., and A. W. Stelson, Aqueous phase chemical processes in deliquescent sea-salt aerosols: A mechanism that couples the atmospheric cycles of S and seasalt, *J. Geophys. Res.*, *97*, 20565-20580, 1992.

Charlson, R.J., J.E. Lovelock, M.O. Andreae, and S.G. Warren, Oceanic phytoplankton, atmospheric sulfur, cloud albedo and climate, *Nature*, *326*, 655, 1987.

Demore, W.B., S.P. Sander, D.M. Golden, R.F. Hampson, M.J. Kurylo, C.J. Howard, A.J. Ravishankara, C.E. Kolb, and M.J.Molina, Chemical kinetics and photochemical data for use in stratospheric modeling, Evaluation 10, *JPL Publ.*, 92-20, 1992.

Gallagher, M.S., D.B. King, P.-Y. Whung, and E.S. Saltzman, Performance of the HPLC/Fluorescence SO_2 Detector during the GASIE instrument intercomparison experiment, submitted to *J. Geophys. Res.*, *102*, 16247-16254, 1997.

Hainsworth, A. H. W., A. L. Dick, and J.L. Gras, Climatic context of ACE 1: A meteorological and chemical overview, *J. Geophys. Res.*, this issue.

Hegg, D.A., The importance of liquid-phase oxidation of SO_2 in the troposphere, *J. Geophys. Res.*, *90*, 3773-3780, 1985.

Hicks, B.B., and P.S. Liss, Transfer of SO_2 and other reactive gases across the air-sea interface, *Tellus*, *28*, 348-354, 1976.

Hynes, A.J., P. Wine, and D.H. Semmes, Kinetics and mechanism of OH reactions with organic sulfides, *J. Phys. Chem.*, *90*, 4148-4156, 1986.

Keller, M.D., W.K. Bellows, and R.L. Guillard, Dimethyl sulfide production in marine phytoplankton, in *Biogenic Sulfur in the Environment*, *ACS Symp. Ser.*, vol. 393, 167-182, edited by E.S. Saltzman and W.J. Cooper, pp. 167-182, ACS Books, Washington, D.C., 1989.

Koga, S., and H. Tanaka, Numerical study of the oxidation process of dimethylsulfide in the marine boundary layer, *J. Atmos. Chem.*, *17*, 201-228 ,1993.

Kok, G. L., A. S. H. Prevot, R.D. Schillawski, and J. E. Johnson, Carbon monoxide measurements from 76°N to 59°S and over the South Tasman Sea, *J. Geophys. Res.*, this issue.

Liss, P.S., Gas transfer: Experiments and geochemical implications, in Air-Sea Exchange of Gases and Particles, edited by P. S. Liss and W. G. N. Slinn, PP. 241-298, D. Reidel, Norwell, Mass., 1983.

Monahan, E.C., The ocean as a source for atmospheric particles, in The Role of Air-Sea Exchange in Geochemical Cycling, edited by P. Buat-Menard, pp. 129-163, D. Reidel, Norwell, Mass., 1986.

Putaud, J.P., N. Mihalopoulos, B.C. Nguyen, J. M. Campin, and S. Belviso, Seasonal variations of atmospheric sulfur dioxide and dimethylsulfide concentrations at Amsterdam Island in the southern Indian Ocean, *J. Atmos. Chem.*, *15*, 117-131, 1992.

Saltzman, E. S., and D. J. Cooper, Shipboard measurements of atmospheric dimethyl sulfide and hydrogen sulfide in the Caribbean and Gulf of Mexico, *J. Atmos. Chem.*, *7*, 191-209, 1988.

Saltzman E.S., S.A. Yvon, and P.A. Matrai, Low level detection of atmospheric sulfur dioxide measurements using HPLC/Fluorescence detection, *J. Atmos. Chem.*, *17*, 73-90, 1993.

Shaw, G.E., Bio-controlled thermostasis involving the sulfur cycle, *Clim. Change*, *5*, 297-303, 1983.

Spivakovsky, C.M., R. Yevich, J.A. Logan, S.C. Wofsy, M.B. McElroy, and M.J. Prather, Tropospheric OH in a three-dimensional chemical tracer model: An assessment based on observations of CH_3CCL_3, *J. Geophys. Res.*, *95*, 18441-18471, 1990.

Turnipseed, A.A., and A. R. Ravishankara, The atmospheric oxidation of dimethylsulfide: Elementary steps in a complex mechanism, in Dimethylsulfide: Oceans, Atmosphere and Climate, edited by G. Restelli and G. Angeletti, pp. 185-195, Kluwer Acad., Norwell, Mass., 1993.

Turnipseed, A.A., S. B. Barone, and A.R. Ravishankara, Reaction of OH with dimethyl sulfide, 2, Products and mechanisms, *J. Phys. Chem.*, *100*, 14703-14713, 1996.

Wanninkhof, R., Relationship between wind speed and gas exchange over the ocean, *J. Geophys. Res.*, 7373-7382, 1992.

Warneck, P., Chemistry of the Natural Atmosphere, edited by R. Dmowska and J. Holton, pp. 313-323, Academic, San Diego, Calif., 1988.

Yin, F., D. Grosjean, and J. H. Seinfeld, Photo-oxidation of dimethyl sulfide and dimethyl disulfide, I, Mechanism development, *J. Atmos. Chem.*, *11*, 1990, 309-364, 1990a.

Yin, F., D. Grosjean, and J. H. Seinfeld, Photo-oxidation of dimethyl sulfide and dimethyl disulfide, II, Mechanism evaluation, *J. Atmos. Chem.*, *11*, 365-399, 1990b.

Yvon, S.A., and E.S. Saltzman, A time-dependent photochemical box model for marine and atmospheric chemistry (PBMAC), RSMAS *Tech. Rep. 93-008*, 77 pp., Univ. of Miami, Miami, Florida, 1993.

Yvon, S.A., and E.S. Saltzman, The sulfur dioxide budget in the tropical South Pacific marine boundary layer (12°S, 135°W), *J. Geophys. Res.*, *101*, 6911-6918, 1996.

Yvon, S.A., E.S. Saltzman, D.J. Cooper, T.S. Bates, and A.M. Thompson, Atmospheric dimethylsulfide cycling at a tropical South Pacific station (12°S, 135°W): A comparison of field data and model results, *J. Geophys. Res.*, *101*, 6899-6909, 1996.

T.S. Bates, PMEL, NOAA, Seattle, WA 98115.

J. M. Cainey, CSIRO Atmospheric Research, Aspendale, Victoria 3195, Australia.

W.J. DeBruyn and E. S. Saltzman, Rosenstiel School of Marine and Atmospheric Science, University of Miami, Miami, FL 33149. (e-mail: debruyn@oj.rsmas.miami.edu)

(Received August 8, 1997; revised March 2, 1998;
accepted March 9, 1998.)